Superfocusing of high-M^2 semiconductor laser beams: experimental demonstration

G.S.Sokolovskii[a], V.Melissinaki[b], V.V.Dudelev[a], S.N.Losev[a], K.K.Soboleva[c], E.D.Kolykhalova[a], A.G.Deryagin[a], V.I.Kuchinskii[a], E.A.Viktorov[d,e], M.Farsari[b], W.Sibbett[f], E.U.Rafailov[g]

[a] Ioffe Physical-Technical Institute, St. Petersburg, Russia
[b] IESL-FORTH, Heraclion, Greece
[c] St. Petersburg State Polytechnical University, St. Petersburg, Russia
[d] Univerite libre de Bruxelles, Brussel, Belgium
[e] National Research University of Information Technologies, Mechanics and Optics, St. Petersburg, Russia
[f] University of St. Andrews, St. Andrews, UK
[g] Aston Institute of Photonic Technologies, Aston University, Birmingham, UK

ABSTRACT

The focusing of multimode laser diode beams is probably the most significant problem that hinders the expansion of the high-power semiconductor lasers in many spatially-demanding applications. Generally, the 'quality' of laser beams is characterized by so-called 'beam propagation parameter' M^2, which is defined as the ratio of the divergence of the laser beam to that of a diffraction-limited counterpart. Therefore, M^2 determines the ratio of the beam focal-spot size to that of the 'ideal' Gaussian beam focused by the same optical system. Typically, M^2 takes the value of 20-50 for high-power broad-stripe laser diodes thus making the focal-spot 1-2 orders of magnitude larger than the diffraction limit. The idea of 'superfocusing' for high-M^2 beams relies on a technique developed for the generation of Bessel beams from laser diodes using a cone-shaped lens (axicon). With traditional focusing of multimode radiation, different curvatures of the wave-fronts of the various constituent modes lead to a shift of their focal points along the optical axis that in turn implies larger focal-spot sizes with correspondingly increased values of M^2. In contrast, the generation of a Bessel-type beam with an axicon relies on 'self-interference' of each mode thus eliminating the underlying reason for an increase in the focal-spot size. For an experimental demonstration of the proposed technique, we used a fiber-coupled laser diode with M^2 below 20 and an emission wavelength in ~1µm range. Utilization of the axicons with apex angle of 140deg, made by direct laser writing on a fiber tip, enabled the demonstration of an order of magnitude decrease of the focal-spot size compared to that achievable using an 'ideal' lens of unity numerical aperture.

Keywords: Bessel beam, superfocusing, diffraction limit.

1. INTRODUCTION

Non-diffracting (Bessel) light beams, that are capable of retaining their intensity during propagation, were reported in 1987 by Durnin [1] (and by Zel'dovich et al. and by McLeod as early as in the 1950s-60s [2,3]) and called Bessel beams because their amplitude profiles can be described by a zero-order Bessel function of the first kind. In a projection onto a transverse plane (perpendicular to the propagation direction) such a beam appears as a bright spot surrounded by concentric fringes. Bessel beams are generated through the interference of convergent beams taking place when a collimated Gaussian beam transits a cone-shaped lens (axicon). The central spot diameter of the Bessel beam is determined by the axicon angle and can be of the order of the optical wavelength. In practice, Bessel beams exhibit a finite propagation distance that depends on the cross-sectional diameter of the initial collimated beam. Another remarkable property of Bessel beams is the ability of the central ray to self-reconstruct its profile when disturbed by an obstacle [4]. Until recently, it was believed that only lasers exhibiting high coherence (gas or solid state lasers) could be used to produce Bessel beams. However, recent work has shown that Bessel beams can be produced from different semiconductor light sources, including light emitting diodes (LED) [5], edge- emitting laser diodes [5,6], vertical cavity

surface emitting lasers (VCSEL) [5, 7, 8] and vertical external cavity surface emitting lasers (VECSEL) [7, 8], and even from a halogen bulb [9] (the last with substantial aperturing). These reports open the way for 'direct' implementations of semiconductor lasers. It is well known, that non-diffracting beams are extremely important in biomedical research because of applications involving optical trapping and tweezing [10, 11]. The use of Bessel beams allows the distance between the focusing optics and manipulated objects to be significantly increased and eliminates the need for fine adjustment, thus making micromanipulation systems more flexible and attractive for practical implementations. The utilization of Bessel beams also opens new horizons in microporation [12], Doppler velocity measurement and colloid research [13], manipulation of micro-machines [14] and micro-fabrication [15,16], as well as for frequency doubling and for other nonlinear optical effects [17,18]. In optical coherence tomography (OCT), Bessel beams enable an order of magnitude increase of focusing depth into a sample [19,20], whereas in optical microscopy, these 'needle' beams are capable of producing in-depth 3D images with only 2D scan [21] to facilitate reduced scattering artifacts with increased image quality and penetration depth in dense media [22]. Interestingly, in projection tomography, Bessel beams can be used to image at much greater depths than for confocal microscopy [23].

1. SUPERFOCUSING OF THE QUASI-GAUSSIAN BEAMS WITH HIGH M^2

The main problem that limits direct applications of high-power semiconductor lasers is the relatively low spatial quality of the emitted radiation due to multimode generation and filamentation. In general, the quality of laser beams is conventionally characterized by the beam propagation factor, M^2 [24], This beam propagation parameter M^2 conveniently allows a mathematical representation developed for the Gaussian beams to be applied to the description of the quasi-Gaussian beams by merely replacing the wavelength λ with an M^2 fold quantity ($\lambda \rightarrow M^2 \cdot \lambda$). E.g. the focal radius of the quasi-Gaussian beam ω_0 is then given by:

$$\omega_0 = \frac{M^2 \lambda}{\pi NA} \tag{1}$$

where NA is the numerical aperture.

Typically, the values for M^2 for high-power broad-stripe laser diodes fall in the range of 20-50. Thus the focal-spot size for the quasi-Gaussian beam emitted by such a laser is typically one or even two orders of magnitude higher than the diffraction-limited value. To overcome this limitation, we recently proposed a method of the 'interference' focusing of the multimode semiconductor laser radiation [25]. The idea of such a 'superfocusing' relies on the technique developed for generation of Bessel beams with laser diodes.

Let us consider Bessel beam produced by an axicon with the apex angle α and refractive index n. The radius of the central lobe of the Bessel beam generated from the plane wave with such an axicon is given by the well-known expression [26]:

$$r_0 \approx \frac{\kappa \lambda}{2\pi (n-1)\cos{\alpha/2}} \tag{2}$$

where κ is the dimensionless coefficient defining the level of intensity merging the central lobe from the first dark ring of the Bessel beam ($\kappa = 2.4$ corresponds to the first zero of Bessel function, $\kappa = 1.75$ corresponds to the $1/e^2$ level of maximum and $\kappa = 1.13$ corresponds to the half-width at half-maximum). If we now consider the generation of a Bessel beam from the quasi-Gaussian one, its divergence can not be neglected and expression (2) transforms to the form:

$$r_{M^2} \approx \frac{\kappa \lambda}{2\pi (n-1)\cos\left(\alpha/2 - x(z)\right)} \tag{3}$$

that takes into account the angle of divergence of the initial quasi-Gaussian beam $x(z)$. This angle can be determined as the ratio of the z coordinate of the refracted beam to the wavefront curvature of the initial quasi-Gaussian beam at that point and takes the form [26]:

$$x(z) = \frac{n-1}{2} \frac{\pi - \alpha}{1 + \left(\frac{\pi R_0^2}{M^2 \lambda z}\right)^2} \tag{4}$$
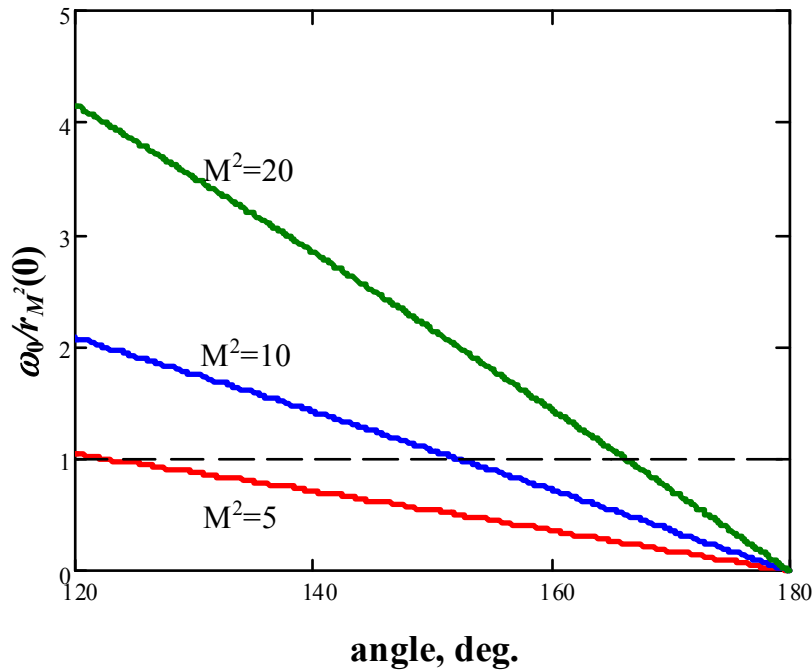
Figure 1. Figure of merit for superfocusing of high-M^2 quasi-Gaussian beam vs axicon angle for the beam propagation parameter values M^2=5 (red), 10 (blue), 20 (olive). Black dashed line indicates the level $\omega_0 = r_{M^2}(0)$.

where R_0 is radius of the collimated quasi-Gaussian beam incident to the axicon. Substituting (4) into (3) one can write expression for the radius of the central lobe of the Bessel beam r_{M^2} versus propagation distance z:

$$r_{M^2}(z) \approx r_0 \left[1 + \left(\frac{M^2 \lambda z}{\pi R_0^2} \right)^2 \right] \tag{5}$$

From (5) it is clear that the central lobe size of the Bessel beam generated form the quasi-Gaussian one r_{M^2} can be very close to that of the plane-wave-generated counterpart r_0 near the axicon tip. So, the figure of merit for superfocusing of the high-M^2 quasi-Gaussian beam is simply the ratio of the 'normal' beam waist size ω_0 when focused with the unity numerical aperture NA=1 to the minimum central lobe size achievable with the interference focusing:

$$\frac{\omega_0}{r_{M^2}(0)} = \frac{2M^2}{\kappa NA} \cdot (n-1)\cos \frac{\alpha}{2}. \tag{6}$$

The figure of merit for superfocusing of high-M^2 quasi-Gaussian beam versus the axicon apex angle is shown in fig.1. Red, blue and olive curves are plotted for the beam propagation parameter values M^2=5, 10 and 20 correspondingly. The dashed black line indicates the level $\omega_0 = r_{M^2}(0)$, so the curves above the dashed line correspond to superfocusing. From fig 1 it is clear that high-M^2 quasi-Gaussian beam can be 'interference' focused by an axicon to the focal spot with size which is much smaller comparing to that achievable when focused with an 'ideal' lens of unity numerical aperture.

2. EXPERIMENT

When a physical axicon is considered, one should be aware of the rounding of its apex which is almost unavoidable for all commercially available conically-shaped lenses. Typically, the radius of rounding is not large (~100 μm) and the size of the rounded area is below 50 μm for any high-end conical lens, so its influence is not important for many applications. However, the rounding of the axicon apex compromises the axicon performance when used for superfocusing because it enlarges the minimal achievable size of the central lobe of the Bessel beam [26]. So, the sharpness of axicon tip is an important condition for an experimental demonstration of superfocusing.
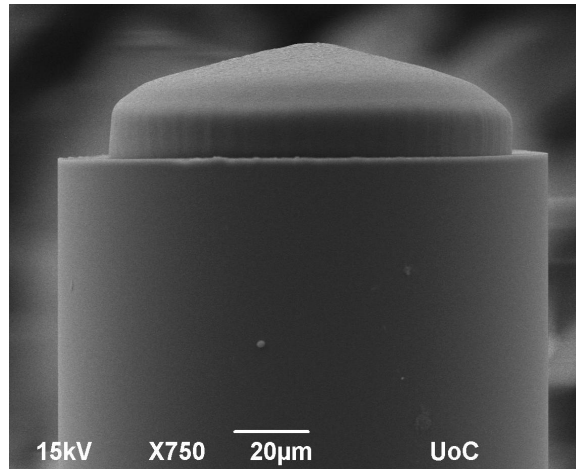
Figure 2. SEM image of the microaxicon manufactured on the tip of the optical fiber. The axicon apex angle is 140^0.

The axicons used in our experiments were fabricated by direct laser writing (DLW) using multi-photon polymerization [27] on the edge of the optical fiber with 100 μm core.The experimental set-up, specially adapted for the fabricated on fiber-tip, has been described previously [28]. A Ti:sapphire femtosecond laser beam (Femtolasers Fusion, 800 nm, 75MHz, <20fs) was focused into the photopolymer using a high numerical aperture microscope objective lens (40x, N.A. = 0.95, Zeiss, Plan Apochromat). The axicon was designed in SolidWorks® and sliced in 100 nm horizontal slices. Each slice was "written" into the photopolymer by moving the focused laser beam using a galvo scanner (ScanLab), adapted for the microscope objective. Subsequently, the sample was lowered 100nm and the next slice was "written". The z-axis movement was achieved using a linear stage (Physik Instrumente) and the average power used for the fabrication of the axicon structures was 40 mW, measured before the objective, while the average transmission was 20%. The scanning speed was set to200 μm/s.
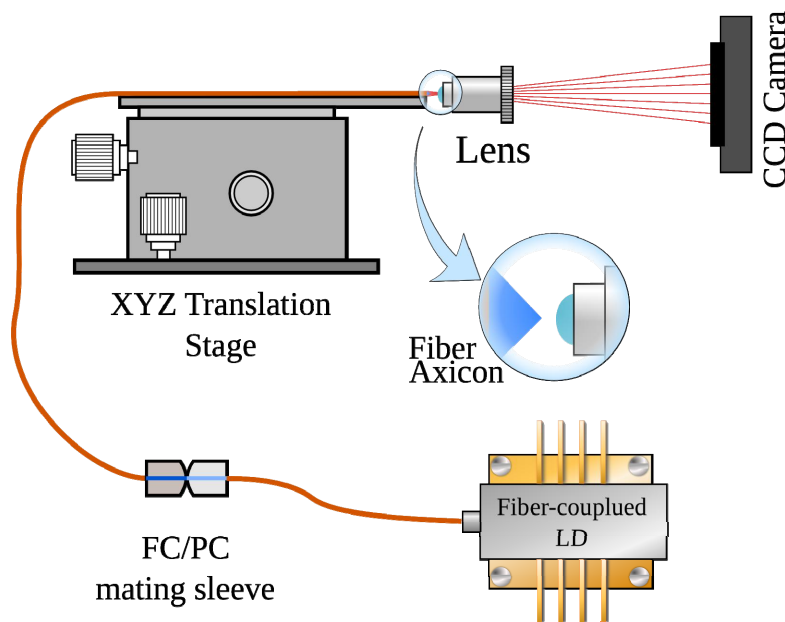

Figure 3. Schematic view of the experimental setup used for demonstration of superfocusing.

The fabrication of the axicon was done using an zirconium-silicon organic-inorganic hybrid composite [29]. Its main components are methacryloxy-propyltrimethoxysilane (MAPTMS), methacrylic acid (MAA) and zirconium *n*-propoxide (ZPO) 70% solution in 1-propanol. The molar ratios were 8:2 for MAPTMS/ZPO and 1:3 for ZPO/MAA. The photoinitiator used was 4,4-bis(diethylamino) benzophenone (Michler's ketone) at a 1% w/w concentration to the final

solution. After DLW processing, the sample was developed and the material not exposed to the laser radiation removed by immersion in a 1:1 isopropanol/1-propanol solution.
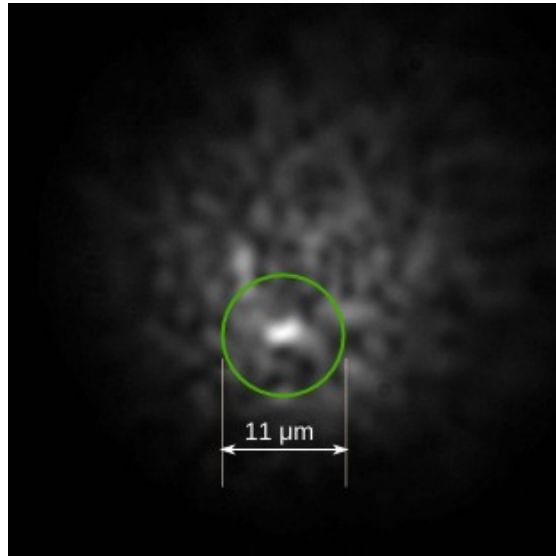

Figure 4. Cross-section of the Bessel beam intensity distribution generated with the fiber microaxicon from 960 nm fiber-coupled semiconductor laser of M^2=18. The size of the central lobe is approximately 2x4 µm (full image size is 50x50 µm). Green circle indicates the minimal achievable focal spot size for such a laser beam if focused with a lens of a unity numerical aperture.

All fiber microaxicons used in our assessments featured a sharp apex with less than 10 µm rounding area and an angle of 140^0. A scanning electron microscopy (SEM) image of the microaxicon on the edge of the optical fiber is shown in fig. 2. The other end of the optical fiber was terminated with FC/PC fiber coupler to eliminate unwanted wavefront distortions on the cleaved fiber tip.
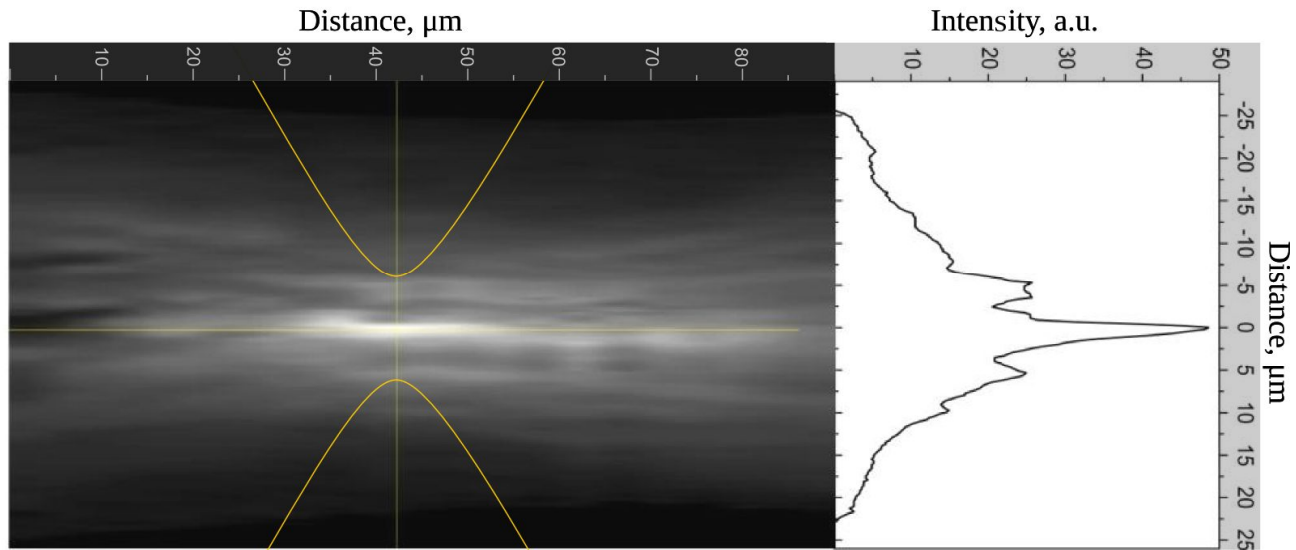

Figure 5. The longitudinal distribution of the Bessel beam intensity produced by the fiber microaxicon from 960 nm fiber-coupled semiconductor laser of M^2=18. The full image size is 90x55 µm. The Bessel beam propagation length is approximately 20 µm and the yellow line profile indicates the ray traces for such a laser beam if focused with a lens of numerical aperture NA=0.85.

The source of a quasi-Gaussian beam for the superfocusing experiments was a fiber-coupled semiconductor laser emitting at 960 nm. The diameter of the fiber core was 100 μm, similar to the fiber axicons used in our experiments. The beam propagation parameter of the laser source at the output from the fiber was measured to be M^2=18 in all range of pumping used in our experiments. The fiber microaxicon was coupled to the laser source with a FC/PC mating sleeve. A microaxicon-edged fiber was mounted on the high-precision xyz-stage enabling fine control of the distance between the axicon tip and the magnifying lens used with CCD camera for registration of the intensity distributions of the generated Bessel beams. The schematic view of the experimental setup is shown in fig.3. The distance between the lens and CCD camera was kept constant to retain the same magnification in all assessments. The size of the image monitored by the camera was calibrated with a graticule placed in the focal plane of the magnifying lens.

The typical image of the laser output superfocused with the microaxicon and registered with CCD camera is shown in fig.4. The size of the bright spot corresponding to the central lobe of the Bessel beam produced with the fiber microaxicon is approximately 2x4 μm. Given the wavelength λ=960 nm and the beam propagation parameter of M^2=18, the minimal achievable focal spot size ω_0 for such a laser beam focused with a lens of unity numerical aperture according to (1) is approximately 11 μm as indicated in fig.4 with green circle.

The transverse profiles of the laser beam intensity distribution were taken with the CCD camera in 5 μm steps. In total, 19 images were taken tos allow the building of a longitudinal distribution of the Bessel beam intensity produced by the fiber microaxicon as shown in fig.5. From this figure, one can estimate the non-diffracting propagation length of such a 'needle' optical beam to be approximately 20 μm, which is an order of magnitude shorter than what could be expected with given aperture and apex angle of the axicon [26]. This reduction of the propagation length is due to remaining rounding of the axicon apex and imperfections of its conical surface, as seen from fig.2. Work on improvingthe quality of the microaxicons is under way and we expect further enhancement of the superfocusing parameters in our future experiments.

3. CONCLUSION

In this paper, we have demonstrated superfocusing of high-M^2 laser beams by technique developed for generation of Bessel beams with an axicon. Significant problems for the demonstration of the superfocusing were the divergence of the laser diode beam when collimated to the axicon and the rounded shape of the axicon apex. Any of these may result in corruption of the Bessel beam and significant increase of the width of its central lobe. The elegant solution for both of these technical problems demonstrated in this work is the utilization of microaxions produced on the tip of the 100um optical fiber with ultrahigh-precision direct laser writing. The fiber axicons used in our assessments featured a rounded area of the apex as small as ~10 μm in diameter and an apex angle of 140^0. This enabled the demonstration of 2 μm to 4 μm focused laser 'needle' beams with approximately 20 μm propagation length generated from multimode laser diode with beam propagation parameter M^2=18 and emission wavelength of 0.96μm which is few-fold reduction compared to the minimal focal spot size of ~11 μm that could be achieved if focused by an 'ideal' lens of a unity numerical aperture.

REFERENCES

[1] J. Durnin, "Exact solutions for nondiffracting beams. I. The scalar theory" J. Opt. Soc. Am. A 4, 651-654 (1987).
[2] B.Ya. Zel'dovich, N.F. Pilipetskii, "Pole lazernogo izlucheniya, sfocussirovanoe realnymi sistemami (in Russian)" Izvestia VUZov Radiophysics 9, 95-101 (1966).
[3] J.H. McLeod, "The Axicon: A New Type of Optical Element" J. Opt. Soc. Am. 44, 592-597 (1954).
[4] Z. Bouchal, J. Wagner, M. Chlup, "Self-reconstruction of a distorted nondiffracting beam" Opt. Commun. 151, 207-211 (1998).
[5] G.S. Sokolovskii, V.V. Dyudelev, S.N. Losev, S.A. Zolotovskaya, A.G. Deryagin, V.I. Kuchinskii, E.U. Rafailov, W.Sibbett, "Generation of propagation-invariant light beams from semiconductor light sources" Tech. Phys. Lett. 34, 1075-1077 (2008).
[6] G.S. Sokolovskii, V.V. Dudelev, S.N. Losev, A.G. Deryagin, D.A. Vinokurov, A.V. Lyutetskii, N.A. Pikhtin, S.O. Slipchenko, I.S. Tarasov, S.A. Zolotovskaya, E.U. Rafailov, V.I. Kuchinskii, W. Sibbett, "Study of non diffracting light beams from broad stripe edge emitting semiconductor lasers" Tech. Phys. Lett. 36, 9-12 (2010).

[7] G.S. Sokolovskii, S.A. Zolotovskaya, S.N. Losev, V.V. Dudelev, A.G. Deryagin, V.I. Kuchinskii, W. Sibbett, E.U. Rafailov, "High power Bessel beams from EP-VECSELs" Proc. SPIE 7919, 79190J, DOI:10.1117/12.877066 (2011).

[8] G.S. Sokolovskii, M. Butkus, S.N. Losev, V.V. Dudelev, A.G. Deryagin, V.I. Kuchinskii, W. Sibbett, E.U. Rafailov, "Non-diffracting beams from surface-emitting lasers" Proc. SPIE 8242, 82420T, DOI: 10.1117/12.907913 (2012).

[9] P. Fischer, C. Brown, J. Morris, C. López-Mariscal, E.Wright, W. Sibbett, K. Dholakia, "White light propagation invariant beams" Opt. Express 13, 6657-6666 (2005).

[10] A. Ashkin, J.M. Dziedzic, "Optical trapping and manipulation of viruses and bacteria" Science 235, 1517-1520 (1987).

[11] V. Garces-Chavez, D. McGloin, H. Melville, W.Sibbett, K. Dholakia, "Simultaneous micromanipulation in multiple planes using a self-reconstructing light beam" Nature 419, 145-147 (2002).

[12] X. Tsampoula, V. Garces-Chavez, M. Comrie, D. J. Stevenson, B. Agate, C.T.A. Brown, F. Gunn-Moore, K. Dholakia, "Femtosecond cellular transfection using a nondiffracting light beam" Appl. Phys. Lett. 91, 053902 (2007).

[13] A.E. Larsen, D.G. Grier, "Like-charge attractions in metastable colloidal crystallites" Nature 385, 230-233 (1997).

[14] M.E.J. Friese, H. Rubinsztein-Dunlop, J. Gold, P. Hagberg, D. Hanstorp, "Optically driven micromachine elements" Appl. Phys. Lett. 78, 547-549 (2001).

[15] J. Amako, D. Sawaki, E. Fujii, "Microstructuring transparent materials by use of nondiffracting ultrashort pulse beams generated by diffractive optics" J. Opt. Soc. Am. B 20, 2562–2568(2003).

[16] M.K. Bhuyan, F. Courvoisier, P.A. Lacourt, M. Jacquot, R. Salut, L. Furfaro, J.M. Dudley, "High aspect ratio nanochannel machining using single shot femtosecond Bessel beams" Appl. Phys. Lett. 97, 081102 (2010).

[17] T. Wulle, S. Herminghaus, "Nonlinear optics of Bessel beams" Phys. Rev. Lett. 70, 1401-1405 (1993).

[18] V.N. Belyi, N.S. Kazak, N.V. Kondratyuk, N.A. Khilo, A.A. Shagov, "Second harmonic generation for Bessel light beams in a KTP crystal" Quantum Electronics 28, 1011-1016 (1998).

[19] Z.H. Ding, H.W. Ren, Y.H. Zhao, J.S. Nelson, Z.P. Chen, "High-resolution optical coherence tomography over a large depth range with an axicon lens" Opt. Lett. 27, 243–245 (2002).

[20] K.S. Lee J.P. Rolland, "Bessel beam spectral-domain high-resolution optical coherence tomography with micro-optic axicon providing extended focusing range" Opt. Lett. 33, 1696–1698 (2008).

[21] P. Dufour, M. Piche, Y.D. Korninck, N. McCarthy "Two-photon excitation fluorescence microscopy with a high depth of field using an axicon" Appl. Opt. 45, 9246–9252 (2006).

[22] F.O. Fahrbach, P.H. Simon, A. Rohrbach, "Microscopy with self-reconstructing beams" Nature Photon. 4, 780–785 (2010).

[23] J. Sharpe, U. Ahlgren, P. Perry, B. Hill, A. Ross, J. Hecksher-Sorensen, R. Baldock, D. Davidson, "Optical projection tomography as a tool for 3D microscopy and gene expression studies" Science 296, 541–545 (2002).

[24] A.E. Siegman, "How to (maybe) measure laser beam quality" OSA Trends in Optics and Photonics Series 17 OSA Annual Meeting (1998).

[25] G.S. Sokolovskii, V.V. Dudelev, S.N. Losev, A.G. Deryagin, V.I. Kuchinskii, W. Sibbett, E.U. Rafailov, "Superfocusing of Mutimode Semiconductor Lasers and Light-Emitting Diodes" Tech. Phys. Lett. 38, 402-404 (2012).

[26] G.S. Sokolovskii, V.V. Dudelev, S.N. Losev, M. Butkus, K.K. Soboleva, A.I. Sobolev, A.G. Deryagin, V.I. Kuchinskii, W. Sibbett, E.U. Rafailov, "Influence of the axicon characteristics and beam quality parameter M^2 on the formation of Bessel beams from semiconductor lasers" Quantum Electronics 43, 423-427 (2013).

[27] M. Malinauskas, M. Farsari, A. Piskarskas, S. Juodkazis, "Ultrafast laser nanostructuring of photopolymers: A decade of advances" Physics Reports 533, 1 (2013).

[28] M. Malinauskas, A. Zukauskas, V. Purlys, A. Gaidukeviciute, Z. Balevicius, A. Piskarskas, C. Fotakis, S. Pissadakis, D. Gray, R. Gadonas, M. Vamvakaki, M. Farsari, "3D microoptical elements formed in a photostructurable germanium silicate by direct laser writing" Optics and Lasers in Engineering, 50 1785-1788, (2012).

[29] A. Ovsianikov, J. Viertl, B. Chichkov, M. Oubaha, B. MacCraith, I. Sakellari, A. Giakoumaki, D. Gray, M. Vamvakaki, M. Farsari, C. Fotakis, "Ultra-Low Shrinkage Hybrid Photosensitive Material for Two-Photon Polymerization Microfabrication" ACS Nano 2, 2257-2262 (2008).